

COSMOLOGICAL ADAPTIVE MESH REFINEMENT

M.L. NORMAN

*Astronomy Department & NCSA
University of Illinois, Urbana, IL 61801*

AND

G.L. BRYAN

*Princeton University Observatory
Princeton, NJ 08544*

Abstract. We describe a grid-based numerical method for 3D hydrodynamic cosmological simulations which is adaptive in space and time and combines the best features of higher order-accurate Godunov schemes for Eulerian hydrodynamics with adaptive particle-mesh methods for collisionless particles. The basis for our method is the structured adaptive mesh refinement (AMR) algorithm of Berger & Collela (1989), which we have extended to cosmological hydro + N-body simulations. The resulting *multiscale hybrid* method is a powerful alternative to particle-based methods in current use. The choices we have made in constructing this algorithm are discussed, and its performance on the Zeldovich pancake test problem is given. We present a sample application of our method to the problem of *first structure formation*. We have achieved a spatial dynamic range $L_{\text{box}}/\Delta x > 250,000$ in a 3D multispecies gas + dark matter calculation, which is sufficient to resolve the formation of primordial protostellar cloud cores starting from linear matter fluctuations in an expanding FRW universe.

1. Introduction

The inclusion of hydrodynamics and atomic and radiation processes into cosmological structure formation simulations is essential for many applications of interest, including galaxy formation, the structure of the intergalactic medium, formation and evolution of X-ray clusters, and cosmic reion-

ization. A key technical challenge in such simulations is obtaining high mass and spatial resolution in collapsing structures within large cosmological volumes. Algorithms employing Lagrangian particles to represent dark matter and gas have a natural advantage in this regard as they automatically place resolution elements where they are needed. Such methods are now well developed and in widespread use. These include the gridless *TreeSPH* method of Hernquist & Katz (1989) and Katz, Weinberg & Hernquist (1996), as well as the grid-assisted P^3M-SPH method (Evrard 1988; Couchman, Thomas & Pierce 1995). Parallel versions of these methods have recently been developed (Davé, Dubinski & Hernquist 1997; Pearce & Couchman 1997) which, when run on massively parallel computers, can integrate $O(10^7)$ particles in hydrodynamic simulations, and as many as 10^9 particles in pure dark matter simulations (Couchman, these proceedings).

We and other members of the Grand Challenge Cosmology Consortium (GC^3) have explored Eulerian hydrodynamics methods as an alternative to SPH in cosmological simulations (Cen 1992; Anninos, Norman & Clarke 1994; Kang et al. 1994; Bryan et al. 1995; Gnedin 1995; Pen 1995). Provided grids can be constructed which achieve the necessary dynamic range (a non-trivial issue, as we shall see), Eulerian methods have a number of distinct advantages over SPH. These are: (1) *speed*: the use of logically regular data structures avoid time-consuming nearest neighbor searches resulting in $\sim 10\times$ higher update rate; (2) *noise*: fluid is represented as a continuum, not discrete particles, eliminating Poisson noise; (3) *density sampling*: because of point (2), low density cells are computed as accurately as high density cells at the same cost; density gradients spanning many orders of magnitude can be accurately simulated with 3-4 cells per decade per dimension. (4) *integral form*: integral conservation laws are straightforward to implement for mass, momentum, energy and magnetic flux which are numerically conservative to machine roundoff. In addition to the above-mentioned advantages which are generic to any Eulerian method, we add the following for higher order Godunov methods such as PPM or TVD: (5) *shock capturing*: shocks are captured in 1-2 cells with correct entropy generation and non-oscillatory shocks; (6) *upwind*: wave characteristics are properly upwinded for higher fidelity and stability; (7) *low dissipation*: the use of higher order-accurate interpolation results in a very low numerical viscosity—important for angular momentum conservation in protogalactic disks. In addition, radiative transfer and MHD is most easily done on a grid. Implicit algorithms generate large sparse matrix equations for which iterative and direct linear systems solvers are available.

In reference to SPH, we mention several disadvantages of traditional Eulerian methods: (1) *resolution*: limited to the grid spacing Δx ; (2) *invariance*: solutions are not strictly translational and rotational invariant

due to the dependence of truncation errors on the relative velocity between fluid and grid and grid orientation.

In the references cited above, various gridding schemes have been explored to reduce truncation error in regions of high density gradients, as invariably arise in structure formation simulations. Here, we describe a powerful method we have developed based on the adaptive mesh refinement (AMR) algorithm of Berger and Colella (1989). The paper is organized as follows. In Sec. 2 we briefly review the elements of Berger’s AMR. In Sec. 3 we describe the modifications we have made to extend AMR to cosmological hydro+N-body simulations. In Sec. 4 we test the method against several standard test problems in numerical cosmology. In Sec. 5 we illustrate the power of AMR in an application to the formation of the first baryonic objects in a CDM-dominated cosmology.

2. Overview of Berger’s AMR

Adaptive mesh refinement (AMR) was developed by Berger and Olinger (1984) to achieve high spatial and temporal resolution in regions of solutions of hyperbolic partial differential equations where fixed grid methods fail. Algorithmic refinements and an application to shock hydrodynamics calculations were described in Berger & Collela (1989). The hydrodynamic portion of our method is based closely on this latter paper, and we refer the reader to it for details (see also paper by Klein et al., these proceedings).

2.1. GRID HIERARCHIES

Unlike some mesh refinement schemes which move the mesh points around “rubber mesh” (e.g., Dorfi & Drury 1987) or subdivide individual cells, resulting in an octree data structure (e.g., Adjerid, S. & Flaherty 1998), Berger’s AMR (also becoming known as *structured* AMR to differentiate it from other flavors) utilizes an adaptive hierarchy of grid patches at various levels of resolution. Each rectangular grid patch (hereafter, simply *grid*) covers some region of space in its *parent grid* needing higher resolution, and may itself become the parent grid to an even higher resolution *child grid*. A general implementation of AMR places no restriction on the number of grids at a given level of refinement, or the number of levels of refinement. The hierarchy of grids can be thought of as a tree data structure, where each leaf is a grid.

Each grid is evolved as a separate initial boundary value (IBV) problem. Initial conditions are obtained by interpolation from the parent grid when the grid is created. Boundary conditions are obtained either by interpolation from the parent grid or by copies from abutting *sibling grids* at the same level. To simplify interpolation, grids are constrained to be aligned

Grid Hierarchy

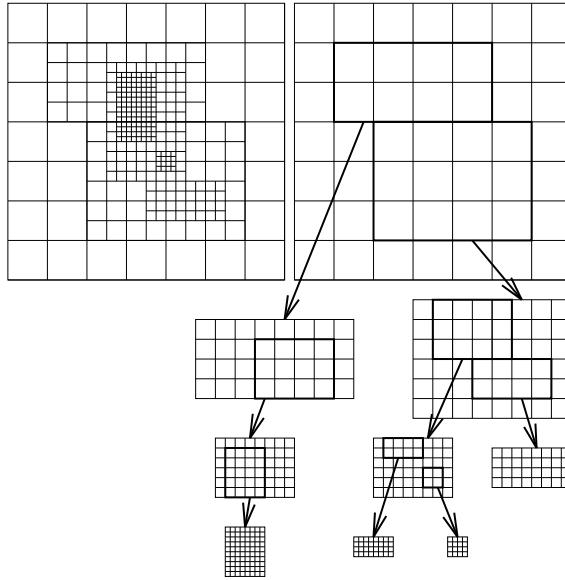


Figure 1. Illustration of an AMR grid hierarchy.

with their parent grid and not overlap their sibling grids. Grids at level ℓ are refined by an integer factor $R_\ell \geq 2$ relative to the grid at level $\ell - 1$. Fig. 1 provides an illustration of these concepts in a 2D, 4-level, $R_\ell = 2$ grid hierarchy.

2.2. ALGORITHM

The algorithm which creates this grid hierarchy is *local* and *recursive*. It can be written in pseudocode as follows. Here `level` is the level of refinement, and procedures are capitalized.

```

Integrate (level)
begin
  if "time for regriding" then Refine(level)
  CollectBoundaryValues(level)

```

```

Evolve (level)
if "level isn't finest existing" then begin
  for r = 1 to R do
    Integrate(level + 1)
    Update(level, level + 1)
  end
end
end

```

Consider a typical calculation which is initialized on a single, coarsely resolved grid called the *root grid*, level $\ell = 0$. The solution is integrated forward in time with procedures `CollectBoundaryValues` and `Evolve`. At each timestep, every cell is checked to determine if it requires refinement—a process known as *selection*. Selection is based either on an estimate of the local truncation error, or some simple threshold criterion, or some Boolean combination thereof. If at least one cell is flagged, then procedure `Refine` is called. It does two things. First, flagged cells are *clustered*, and minimal rectangular boundaries of these clusters are determined using the algorithm of Berger & Rigoustous (1991). Second, one or more refined $\ell = 1$ grids are allocated having these boundaries, and their initial data is computed via interpolation from the root grid. Depending on circumstance, `Refine` may also deallocate unneeded subgrids. The root grid is then advanced one coarse timestep Δt_0 . The $\ell = 1$ subgrids are integrated forward in time with smaller timesteps Δt_1 until they “catch up” with the parent grid. If the hyperbolic system is linear (e.g., advection), then $\Delta t_1 = \Delta t_0/R$, and the refined grids take R timesteps for each coarse grid timestep. However, for nonlinear systems like gas dynamics, fine grid timesteps are determined by the Courant stability condition, and in general $R+1$ timesteps are needed to match times. This detail is not reflected in the pseudocode above. After the fine grids have been advanced to time $t + \Delta t_0$, procedure `Update` is called. It does two things. First, it injects the results of the fine grid calculation into the overlying coarse grid cells through summation or interpolation. Second, the values of coarse grid conserved quantities in cells adjacent to fine grid boundaries are modified to reflect the difference between the coarse and fine grid fluxes—a procedure known as *flux correction*.

The algorithm described above is recursive, and applies to any level in the grid hierarchy. In a multilevel grid hierarchy, the temporal integration scheme is analogous to the “W-cycle” in classic elliptic multigrid. Grids are advanced from coarse to fine with their individually determined timesteps. This order allows us to achieve second order accuracy in time on the entire hierarchy. This is accomplished by interpolating the boundary values not only in space but in time as well using time level n and $n+1$ values on the parent grid.

3. Cosmological AMR

Cosmological hydrodynamic simulations require a robust fluid solver capable of handling the extreme conditions of structure formation, as well as a method for evolving collisionless particles (dark matter, stars) subject to their self-consistent gravitational field, the latter requiring a solution of the Poisson equation. We briefly describe these methods here. A more detailed paper is in preparation (Bryan & Norman 1998).

3.1. COSMOLOGICAL PPM

Our fluid solver is based on the piecewise parabolic method (PPM) of Collela & Woodward (1984), suitably modified for cosmological flows. The algorithm is completely described in Bryan et al. (1995), so we merely state the essential points. PPM is a higher order-accurate version of Godunov's method, featuring third order-accurate piecewise parabolic monotonic interpolation and a nonlinear Riemann solver for shock capturing. Multidimensional schemes are built up by directional splitting, where the order of the 1D sweeps is permuted à la Strang (1968), resulting is a scheme which is formally second order-accurate in space and time. For cosmology, the conservation laws for the fluid mass, momentum, and energy density are written in comoving coordinates for a FRW spacetime with metric scale factor $a(t)$. Both the gas internal energy equation and total (internal + kinetic) energy equation are solved everywhere on the grid at all times. This *dual energy formulation* is adopted in order to have a scheme that both produces the correct entropy jump at strong shocks *and* yields accurate pressures and temperatures in the hypersonic parts of the flow. Both the conservation laws and the Riemann solver must be modified to include gravity. In order to maintain second order accuracy in time, the gravitational potential ϕ is needed at the half time level $t^{n+\frac{1}{2}}$. We use a predictor-corrector approach, wherein the particles are advanced to $t^{n+\frac{1}{2}}$ using ϕ^n , and then $\phi^{n+\frac{1}{2}}$ is computed by solving the Poisson equation, as described below. We have implemented both Lagrange + Remap (LR) and Direct Eulerian (DE) variants of our method, following the example of Collela & Woodward (1984), with comparable results. For AMR applications, we use the DE version to simplify the flux correction step.

3.2. ADDING COLLISIONLESS PARTICLES

Adding collisionless particles to AMR presents two challenges, one physical (how do they interact with the fluid in the mesh), and one algorithmic (how to add a new data structure.) A third challenge—how to compute

the gravitational interaction between the two components in a consistent fashion—is described in the following section.

Our method utilizes a single set of particles with comoving positions \vec{x}_i , proper peculiar velocities \vec{v}_i and masses m_i (other characteristics may be added as needed). There is a unique, one-to-one association between particle i and a grid j at level ℓ $G_{\ell,j}$ if that particle’s position lies within the grid’s boundary but outside of any finer (child) grid. In other words, a particle belongs to the finest grid which contains it. We exploit this association by denoting that grid as the particle’s *home* grid and store all such particles in a list along with the rest of the data connected to that grid. Note that a particle’s home grid may change as it moves, requiring redistribution of particles. This disadvantage is offset by a number of factors, including (1) decreased search time for particle-grid interactions; (2) improved data encapsulation; and (3) better parallelization characteristics (see below). This association is also very natural from a physical standpoint: because the particles are indirectly connected to the solution on their home grid, they tend to share the same timestep requirement.

The particles obey Newton’s equations, which in the comoving frame are:

$$\frac{d\vec{x}_i}{dt} = \frac{1}{a}\vec{v}_i, \quad (1)$$

$$\frac{d\vec{v}_i}{dt} = -\frac{\dot{a}}{a}\vec{v}_i - \frac{1}{a}(\vec{\nabla}\phi)_i \quad (2)$$

where the subscript i in the last term in Eq. 2 means the gravitational acceleration is evaluated at position \vec{x}_i . The gravitational potential is computed from a solution of the Poisson equation, which takes the form in comoving coordinates:

$$\nabla^2\phi = \frac{4\pi G}{a}(\rho - \bar{\rho}), \quad (3)$$

where ρ is the local comoving mass density of gas and particles, and $\bar{\rho}$ is its global average value.

These equations are finite-differenced and solved with the same timestep as the grid, to reduce bookkeeping. Eq. (1) can be solved relatively simply since only quantities local to the particle are involved. We use a predictor-corrector scheme to properly time center the RHS. Eq. (2) requires knowing the gravitational acceleration at position \vec{x}_i . This is accomplished using the particle-mesh (PM) method (e.g., Hockney & Eastwood, 1980). In the first step, particle masses are assigned to the grid using second order-accurate TSC (Triangular Shaped Cloud) interpolation. In the second step, the gridded particle density is summed with the gas density, and then Eq. (3) is solved on the mesh as described below. Finally, in the third step, gravi-

tational accelerations are interpolated to the particle positions using TSC interpolation, and particle velocities are updated.

3.3. SOLVING THE POISSON EQUATION

The description above glossed over an important detail. Namely, that the gravitational field cannot be solved grid by grid, but must have knowledge of the mass distribution on the entire grid hierarchy. However, we wish to use the high spatial resolution afforded by the refined grids to compute accurate accelerations. This is accomplished using a method similar to that set out in Couchman (1991). The basic idea is to represent the acceleration on a particle as the sum of contributions from each level of the hierarchy less than or equal to the level of its home grid:

$$\vec{a}_i = \sum_{\ell'=0}^{\ell} \vec{a}_i(\ell') \quad (4)$$

where the partial accelerations $\vec{a}_i(\ell)$ are computed symbolically as follows:

$$\{\vec{x}_i, m_i\}_{G_\ell} \xrightarrow{TSC} \rho_\ell(\vec{x}_{G_\ell}) \xrightarrow{FFT} \hat{\rho}_\ell(\vec{k}), \quad (5)$$

$$\hat{\phi}_\ell(\vec{k}) = \hat{\rho}_\ell(\vec{k}) \mathcal{G}_\ell(\vec{k}) \longrightarrow \hat{a}_\ell(\vec{k}), \quad (6)$$

$$\hat{a}_\ell(\vec{k}) \xrightarrow{3FFTs} \vec{a}_\ell(\vec{x}_{G_\ell}) \xrightarrow{TSC} \vec{a}_\ell(\vec{x}_i). \quad (7)$$

In the first step, the mass of *all* particles whose positions lie inside the boundaries of grid G_ℓ is assigned to the grid using TSC interpolation, and its Fourier transform is computed. In the second step the Poisson equation is solved in Fourier space using a shaped force law $\mathcal{G}_\ell(\vec{k})$ designed to reproduce a $\frac{1}{r}$ potential when summed over all levels. Accelerations on the grid are computed in Fourier space, and then transformed back into real space in step 3. This requires three FFTs—one for each component. Finally, the acceleration on particle i due to G_ℓ is computed using TSC interpolation. The acceleration on the fluid is computed by treating each cell as a particle with its position given by the center of mass (as determined by a tri-linear interpolation). The assignment of mass and interpolation of acceleration is done with the same TSC scheme as used for the particles.

3.4. REFINEMENT FACTOR AND CRITERIA

In our implementation, the refinement factor R_ℓ can have any integer value, and can be different on different levels. However, we have found through experimentation that $R_\ell = R = 2$ is optimal for cosmological simulations where the gravitational dynamics is dominated by dark matter. Since dark

matter is represented by a fixed number of particles, the use of higher refinement factors $R \geq 3$ refines the gas grid to the point where each dark matter particle becomes an accretion center. The choice $R=2$ maintains commensurate mass resolution in both gas and dark matter.

In order to reduce Poisson noise, we initialize a calculation with one particle per cell. We flag a cell for refinement when the baryonic mass has increased by a factor of four over its initial value. Immediately after refinement, refined cells in 3D have one half their initial mass and typically contain zero or one particle. Thus, in a collapsing structure, the ratio of baryonic to dark matter mass will vary between one half and four times its initial value.

3.5. IMPLEMENTATION

Our implementation features arbitrary refinement factors R_ℓ , number of grids N_g , grid shapes ($n_x \neq n_y \neq n_z$), and grid hierarchy depth ℓ_{max} . We also have the option, not yet exercised, of calling different physics solvers on different levels. The AMR driver is written in object-oriented C++ to simplify logic and memory management. The grid objects encapsulate the grid data (field and particle) as well as numerous grid methods (e.g., `Evolve`). The floating-point intensive methods are implemented in F77 for the sake of computational efficiency. C wrappers interface the C++ and F77 code. Our production version is a shared memory, loop parallel version, where all grids at a given level are executed in parallel. A distributed memory version, wherein the root grid is domain decomposed, is under development.

4. Tests

We have extensively tested our code against a variety of hydrodynamic and hybrid (hydro + N-body) test problems. These include (1) linear waves and shock waves entering and exiting static subgrids in 1D and 2D at various angles; (2) a stationary shock wave in a static 3D subgrid “Shock in a Box” (Anninos, Norman & Clarke 1994); (3) Sod shock tube; (4) 1D pressureless collapse; (5) 1D Zeldovich pancake; (6) 2D pure baryonic CDM model (Bryan et al. 1995); (7) 3D adiabatic X-ray cluster “Santa Barbara cluster” (Frenk et al. 1998); and (8) 3D self-similar infall solution (Bertschinger 1985). In tests, (3-7) AMR results were compared with unigrid results up to grid sizes of 512^3 . In all cases the algorithm performs well, reproducing the reference solutions with a minimum of artifacts at coarse/fine grid interfaces. The use of upwind, second-order accurate fluxes in space and time is found to be essential in minimizing reflections. Details are provided in Bryan & Norman (1998).

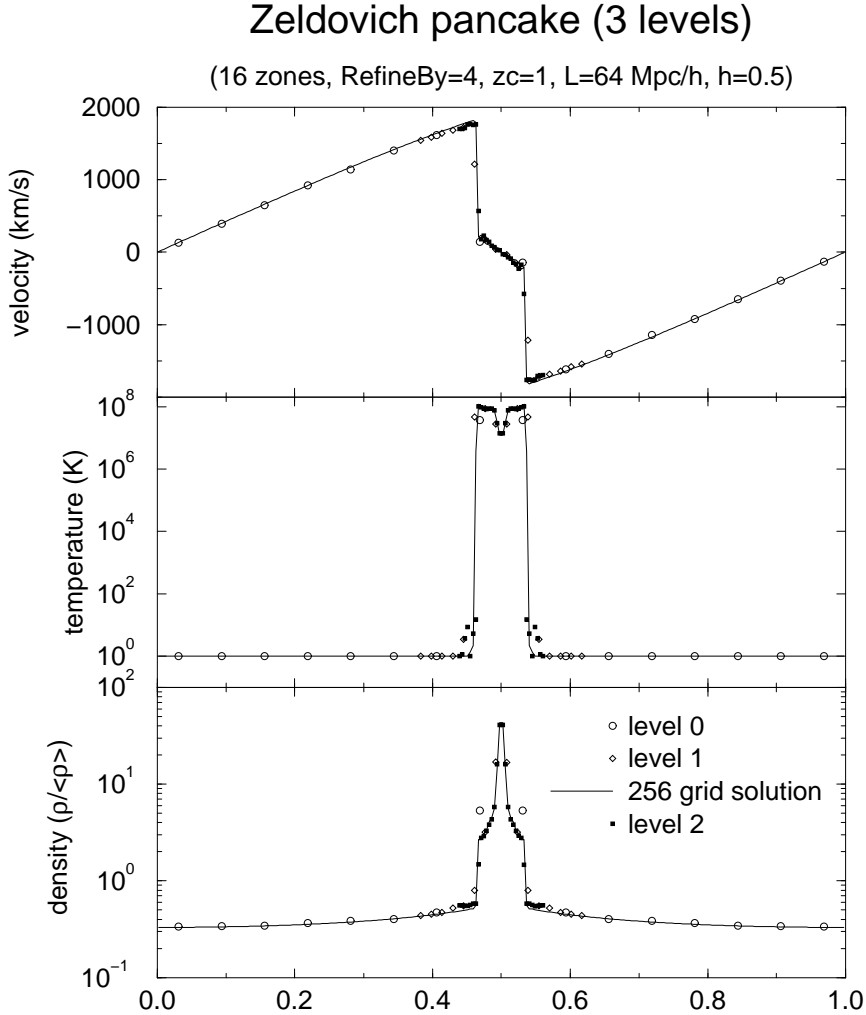


Figure 2. 1D Zeldovich pancake test problem. 3-level solution (symbols) is overlaid on 256 zone uniform grid solution (solid line).

As an example, Fig. 2 shows the code’s performance on the 1D Zeldovich pancake test problem. The parameters for this problem, which includes gas, dark matter, gravity, and cosmic expansion, are given in Bryan et al. 1995. Here we compare a 3-level AMR calculation with a 256 zone uniform grid calculation. The root grid has 16 zones, and the refinement factor $R=4$ (in 1D problems one has more latitude with R .) Thus, the AMR calculation has the same 256 zone resolution on the finest grid $\ell = 2$. We can see that the AMR algorithm places the refinements only in the central high density pancake. The solutions on the three levels of refinement match

smoothly in the supersonic infalling envelope. The density maximum and the local temperature minimum at the midplane agree with the uniform grid results exactly. The shock waves at $x=.45$ and $.55$ are captured in two cells without post-shock oscillations. The temperature field—the most difficult to get right—exhibits a small bump upstream of the shock front. This is caused by our dual energy formulation, and marks the location where we switch from internal energy to total energy as a basis for computing pressures and temperatures. The bump has no dynamical effect as ram pressure dominates by many orders of magnitude ahead of the shock.

5. A Sample Application: First Structure Formation

We have applied our code to the formation of X-ray clusters (Bryan & Norman 1997), galaxy formation (Kepner & Bryan 1998), and the formation of the first baryonic structures in a CDM-dominated universe (Abel, Bryan & Norman 1998). In Fig. 3 we show a result from the latter calculation to illustrate the capabilities of our method.

Our ultimate goal is to simulate the formation of the first stars in the universe (Population III stars) starting from cosmological initial conditions. To resolve the protostellar cloud cores which form these stars requires a spatial dynamic range of at least five orders of magnitude in 3D. The primary coolant in zero metallicity gas for $T < 10^4 K$ is H_2 line cooling (e.g., Tegmark et al. 1997). H_2 forms in the gas phase via nonequilibrium processes (McDowell 1961; Saslaw & Zipoy 1967). Thus, in addition to gas and dark matter, we also solve a 9-species nonequilibrium chemical network for $H, H^+, He, He^+, He^{++}, H^-, H_2^+, H_2$ and e^- in every cell at every level of the hierarchy. This requires adding nine new field variables—one for each species—and solving the stiff reactive advection equations for the coupled network. The physical model is described in Abel et al. (1997). The numerical algorithms for cosmological reactive flow are provided in Anninos et al. (1997).

We simulate a standard CDM model in a periodic, comoving volume 128 kpc on a side. The parameters are: $\Omega_0 = 1, \Omega_b = 0.06, \sigma_8 = 0.7, H_0 = 50$ km/s/Mpc. The starting redshift is $z=100$. The initial conditions are realized on a 3-level static nested grid hierarchy with a root grid resolution of 64^3 cells. The subgrids are centered on the most massive peak which develops. This location is determined by running the simulation once at low resolution. The $\ell = 2$ grid is made large enough so that it initially contains all the mass that eventually ends up in the condensed halo. The initial $\ell = 2$ mass resolution in the gas (dark matter) is $0.5(8)M_\odot$, respectively.

As the calculation proceeds, the AMR algorithm generates many more grids at higher levels of refinement up to a preset limit of 13 levels total.

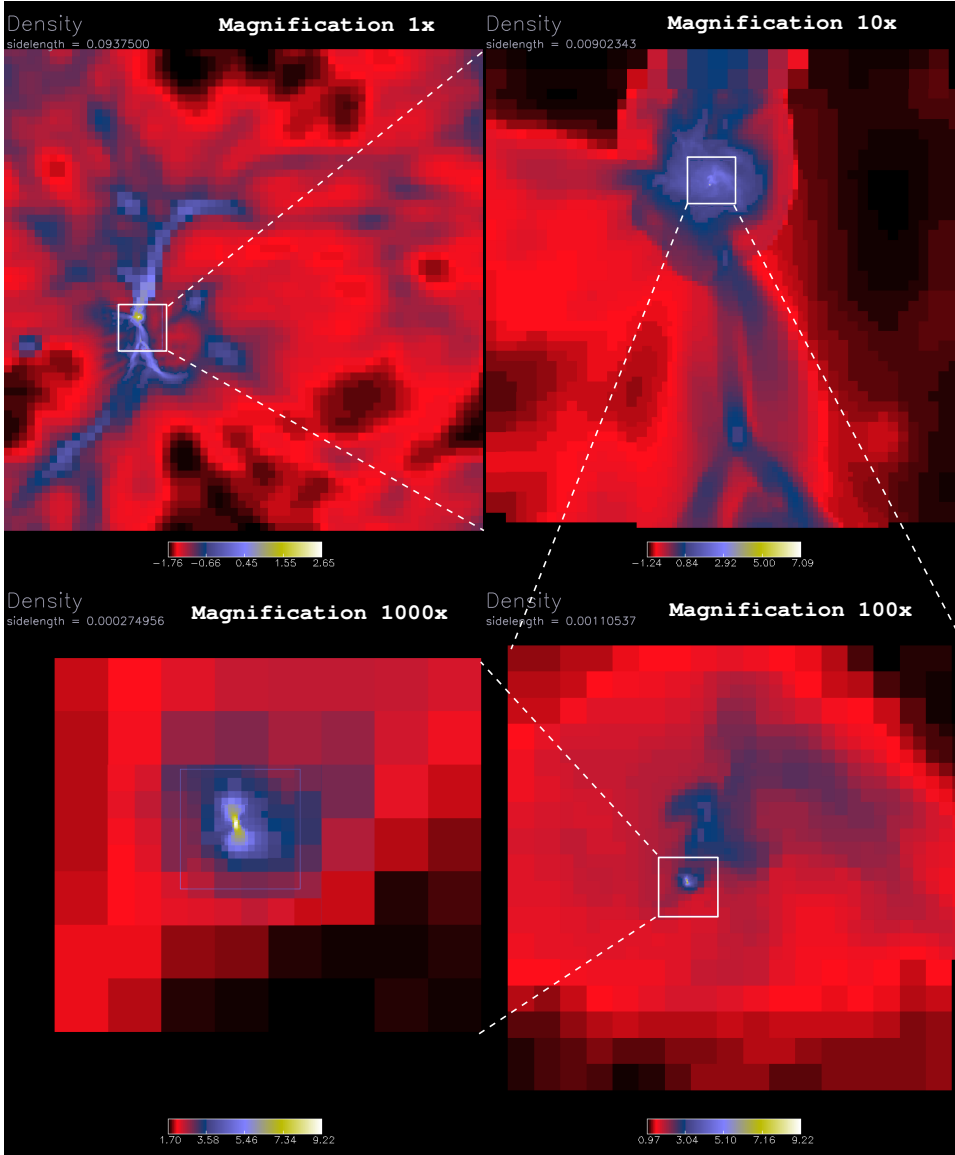


Figure 3. AMR simulation of first structure formation. Plotted at four magnifications is the logarithm of the baryonic overdensity on a slice through the densest structure.

In addition to the overdensity refinement criterion described above, we also require that the numerical Jeans criterion is satisfied everywhere (Truelove et al. 1997; Klein et al. , these proceedings.) Nonlinear structures form in the gas by $z \approx 30$. By $z \approx 20$ sufficient H_2 has formed in the center of the virialized halo that a cooling flow ensues (Abel et al. 1998). Because of

the range of mass scales which go nonlinear nearly simultaneously at these epochs, the halo is quite lumpy as structure builds up hierarchically. By $z = 18$ (Fig. 3), a highly concentrated structure has formed through the collision of two rapidly cooling blobs. A collapsing, primordial protostellar core forms as a result. The core collapses to higher densities, eventually reaching our resolution limit. The proper cell size on the $\ell = 12$ grid is $\Delta x_{12} = 0.025$ pc ~ 5000 AU. The overall dynamic range achieved is $64 * 2^{12} = 262,144$.

We stop the calculation when the Jeans criterion is violated on the $\ell = 12$ grid. This occurs in the densest cell, which has reached a baryonic overdensity of almost 10^{10} and a proper number density of more than 10^8 cm $^{-3}$. At these densities, three body reactions become important, which we have not included in our model. At the end of the calculation, we have formed a parsec-sized collapsing primordial core with about $500M_{\odot}$ of material, roughly equal parts gas and dark matter. The further evolution of this cloud, including the important question of fragmentation, is being studied with a separate, smaller scale AMR simulation in progress.

Acknowledgements We thank our collaborators Tom Abel and Peter Anninos for joint work cited here, as well as Sir Martin Rees for drawing our attention to the problem of first structure formation. This work was carried out under the auspices of the Grand Challenge Cosmology Consortium (*GC³*), with partial funding provided by NSF grant ASC-9318185 and NASA grant NAG5-3923. Simulations were carried out using the SGI Origin2000 at the National Center for Supercomputing Applications, University of Illinois, Urbana-Champaign.

References

- Abel, T., Anninos, P., Zhang, Y. & Norman, M. L. 1997, *New Astronomy*, 2, 181
 Abel, T., Bryan, G. L. & Norman, M. L. 1998. *in preparation*
 Adjerid, S. & Flaherty, J.E. 1998, *SIAM J. of Sci. and Stat. Comp.*, Vol. 9, No. 5, 792
 Anninos, P., Zhang, Y., Abel, T. and Norman, M. L. 1997, *New Astronomy*, 2, 209
 Anninos, P., Norman, M. L. & Clarke, D. A. 1994. *Ap. J.*, 436, 11
 Berger, M. J. & Rigoustous, I 1991. *IEEE Transactions on Systems, Man, Cybernetics*, 21(5).
 Berger, M. J. & Olinger, J. 1984. *J. Comp. Phys.* 53, 484
 Berger, M. J. & Collela, P. 1989. *J. Comp. Phys.* 82, 64
 Bertschinger, E. 1985. *Ap. J. Suppl.*, 58, 39
 Bryan, G. L. & Norman, M. L. 1997. in *Computational Astrophysics*, eds. D. A. Clarke & M. Fall, ASP Conference # 123
 Bryan, G. L. & Norman, M. L. 1998. *in preparation*
 Bryan, G. L., Norman, M. L., Stone, J. M., Cen, R. & Ostriker, J. P. 1995, *Comp. Phys. Comm.*, 89, 149
 Cen, R. 1992, *Ap. J. Suppl.*, 78, 341
 Colella, P. & Woodward, P. R. 1984. *J. Comp. Phys.*, 54, 174

- Couchman, H. 1991. *Ap. J. Lett.* 368, L23
Couchman, H., Thomas, P. & Pierce, F. 1995. *Ap. J.*, 452, 797
Davé, R., Dubinski, J. & Hernquist, L. 1997, *New Astronomy*, 2, 227
Dorfi, E. & Drury, L. 1987. *J. Comp. Phys.*, 69, 175
Evrard, A. E. 1988. *M.N.R.A.S.*, 235, 911
Frenk, C., White, S. *et al.* 1998. *Ap. J.*, *submitted*
Gnedin, N. Y. 1995, *Ap. J. Suppl.*, 97, 231
Hernquist, L. & Katz, N. 1989. *Ap. J. Suppl.*, 70, 419
Hockney, R. W. & Eastwood, J. W. 1980. *Computer Simulation Using Particles*, McGraw-Hill, New York
Kang, H., Cen, R., Ostriker, J. P. & Ryu, D. 1994, *Ap. J.*, 428, 1
Katz, N., Weinberg, D. & Hernquist, L. 1996, *Ap. J. Suppl.*, 105, 19
Kepner, J. & Bryan, G. L. 1998. *in preparation*
McDowell, M. R. C. 1961. *Observatory*, 81, 240
Pearce, F. & Couchman, H. 1997. *New Astronomy*, 2, 411
Pen, U. 1995, *Ap. J. Suppl.*, 100, 269
Saslaw, W.C., Zipoy, D. 1967. *Nature*, 216, 976
Strang, G. 1968. *SIAM J. Num. Anal.*, 5, 506
Tegmark, M., Silk, J., Rees, M.J., Blanchard, A., Abel, T., & Palla, F. 1997. *Ap. J.*, 474,
1
Truelove, J. K. *et al.* 1998. *Ap. J.*, 495, 821